Disentangling the Web of Allosteric Communication in a Homotetramer: Heterotropic Inhibition of Phosphofructokinase from *Bacillus stearothermophilus*†

Allison D. Ortigosa,‡ Jennifer L. Kimmel,‡,§ and Gregory D. Reinhart*

Department of Biochemistry and Biophysics and Center for Advanced Biomolecular Research, Texas A&M University, College Station, Texas 77843-2128

Received June 23, 2003; Revised Manuscript Received October 8, 2003

ABSTRACT: A strategy for isolating each of the four potentially unique heterotropic pairwise allosteric interactions that exist in the homotetramer phosphofructokinase from *Bacillus stearothermophilus* is described. The strategy involves the construction of hybrid tetramers containing one wild-type subunit and three mutant subunits that have been modified to block binding of both the substrate, fructose 6-phosphate (Fru-6-P), and the allosteric inhibitor, phospho(enol)pyruvate (PEP). Each type of binding site occurs at a subunit interface, and mutations on either side of the interface have been identified that will greatly diminish binding at the respective site. Consequently, four different types of mutant subunits have been created, each containing a different active site and allosteric site modification. The corresponding 1:3 hybrids isolate a different pair of unmodified substrate and allosteric sites with a unique structural disposition located 22, 30, 32, and 45 Å apart, respectively. The allosteric inhibition exhibited by the unmodified sites in each of these four hybrids has been quantitatively evaluated in terms of a coupling free energy. Each of the coupling free energies is unique in magnitude, and their relative magnitudes vary with pH. Importantly, the sum of these coupling free energies at each pH is equal to the total heterotropic coupling free energy associated with the tetrameric enzyme. The latter quantity was assessed from the overall inhibition of a control hybrid that removed the homotropic interactions in PEP binding. The results do not agree with either the concerted or sequential models that are often invoked to explain allosteric behavior in oligomeric enzymes.

The basis for allosteric communication within oligomeric proteins for the most part remains an enigma. In part this is due to the inherent complications associated with the multiplicity of ligand binding sites usually present in an oligomer. Even in the simplest homotetramer, containing on average a single active site and a single allosteric site per subunit, no fewer than four potentially unique heterotropic allosteric interactions exist by which the binding of an allosteric ligand can influence the binding of the substrate. To illustrate this point, consider the circumstance of a single equivalent of substrate binding to a tetrameric enzyme to which a single equivalent of allosteric ligand has already bound. There are four different situations that could be encountered since there are four possible sites at which the allosteric ligand could have bound. The question we wish to address is how much of an allosteric effect would be manifested when binding the single equivalent of substrate in each of these four situations.

Assuming the allosteric ligand inhibits substrate binding, one limiting possibility is that it does not matter to which site the allosteric ligand binds; i.e., the allosteric ligand is equally effective at inhibiting the binding of substrate at that single location from any site. Such a result would be predicted by a concerted transition of all subunits to a single inhibited state upon the binding of the first equivalent of inhibitor similar to the concerted model describing allosteric behavior that was originally proposed by Monod et al. (*1*).

Another possibility, representing the other extreme, is that a given active site may be influenced by the binding of an allosteric ligand at only one site. In this situation, binding of an allosteric ligand at any of the other three sites would have no effect. Such a result would be expected if the allosteric sites and the active sites were paired off so that inhibition at each active site was the result of the binding of inhibitor to one particular site, for example, if each subunit was essentially independent of the other. In addition, a sequential model, reminiscent of that proposed by Koshland et al. (*2*), as applied to heterotropic effects would also produce this result when only a single equivalent of each ligand binds, as illustrated in Figure 1.

Reality, of course, may lie somewhere between these extremes, with the binding of an allosteric ligand to each site exerting a unique and varying influence on the binding to a particular active site. Such a circumstance would suggest that multiple heterotropic allosteric routes of communication exist within the tetramer.

This report describes our efforts to measure each of these four potentially unique heterotropic allosteric interactions that can be envisioned in the homotetramer phosphofructokinase from *Bacillus stearothermophilus* (BsPFK)[1] (*3*). BsPFK contains on average one active site and one allosteric site

† This work was supported by National Institutes of Health Grant GM33216 and Robert A. Welch Foundation Grant A1543.

* To whom correspondence should be addressed. Phone: (979) 862-2263. Fax: (979) 845-4295. E-mail: gdr@tamu.edu.

‡ These authors contributed equally to this work.

§ Current address: Department of Biochemistry, University of Missouri−Columbia, Columbia, MO.

10.1021/bi035077p CCC: $27.50
Published on Web 12/16/2003

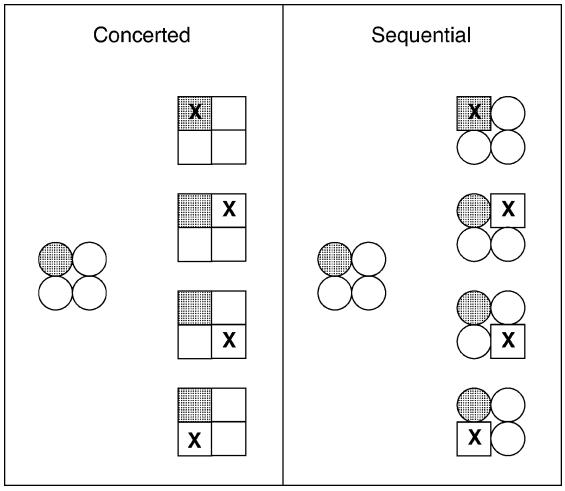

FIGURE 1: Contrasting predictions of simple concerted and sequential models regarding the influence of the binding of a single allosteric ligand to the binding of substrate at a single active site associated with the shaded subunit. In the concerted model, binding of the allosteric ligand, X, to any site influences the binding to the active site to the same degree as commonly denoted by the change in shape from circle to square. In the sequential model, binding to only one site influences the binding of substrate at the shaded site.

per subunit. When PEP binds to the allosteric sites, the affinity for the substrate, Fru-6-P, is diminished. Each of these binding sites spans a subunit−subunit interface, with residues from each side of the interface contributing substantially to the binding energy.

We have previously reported the construction of a 1:3 hybrid enzyme, containing one wild-type subunit and three subunits of a modified form of the enzyme, which isolates a single heterotropic interaction because all but one Fru-6-P and PEP binding site are modified to greatly reduce the affinity of the respective ligand (*5*). We report herein an expansion of this approach in which we have constructed three additional 1:3 hybrids, each of which isolates a different heterotropic interaction. Furthermore, a strong case can be made that each of these isolated interactions relates quantitatively to the corresponding interaction in the native tetramer.

Our results suggest, perhaps not surprisingly, that neither the simplified concerted nor the independent/sequential models properly describe the network of allosteric communication in this enzyme. Rather, the occupancy of each allosteric site by the inhibitor introduces a unique effect on the binding of substrate to a particular active site. The results further suggest that different routes of allosteric communication exist between the various pairwise combinations of allosteric and active sites within the native tetramer.

MATERIALS AND METHODS

Materials. All chemical reagents used for protein purification and kinetic assays were of analytical grade purchased from Sigma-Aldrich, Bio-Rad, or Fisher. The Matrex Blue A−agarose resin used for purification was purchased from Amicon Corp. The coupling enzymes (aldolase, triosephosphate isomerase, and glycerol-3-phosphate dehydrogenase) were purchased as ammonium sulfate suspensions from Roche. Prior to use in kinetic assays, the coupling enzymes were dialyzed extensively against 50 mM MOPS−KOH (pH 7.0), 100 mM KCl, 5 mM $MgCl_2$, and 0.1 mM EDTA. Creatine phosphate, NADH, and the sodium salts of Fru-6-P and PEP were purchased from Sigma-Aldrich. The sodium salt of ATP was obtained from either Sigma-Aldrich or Roche. Creatine kinase was purchased from Roche. Bicinchoninic acid reagents used in determining protein concentration were purchased from Pierce. Site-directed mutagenesis was performed using the Altered Sites in vitro mutagenesis system which was purchased from Promega and included the pALTER vector, pALTER control vector, and ampicillin repair and control oligonucleotides. DNA-modifying enzymes (T4 DNA polymerase, T4 DNA ligase, and T4 polynucleotide kinase) were purchased from Promega. Mutagenesis oligonucleotides were synthesized using an Applied Biosystems 392 DNA/RNA synthesizer at the Gene Technologies Laboratory, Institute of Developmental and Molecular Biology, Texas A&M University. Deionized distilled water was used throughout.

Site-Directed Mutagenesis. All of the BsPFK variants were created via site-directed mutagenesis using the Altered Sites in vitro mutagenesis system as provided by Promega. A pALTER vector, containing the wild-type BsPFK gene under the *lac* promoter termed pGDR26 (*4*), was used to create all of the BsPFK variants. Each mutant protein was created to individually isolate each of the four heterotropic interactions by introducing the various mutations (R162E, R252A, and D12A or R243E at the active site, R25E or R211E/K213E at the allosteric site, and K90E/K91E at the surface of the protein) into the BsPFK gene as described by Kimmel and Reinhart (*5*). All ampicillin-resistant colonies were chosen and sequencing reactions performed across the entire gene to confirm the desired mutations at the Gene Technologies Laboratory via the Sanger dideoxynucleotide method, utilizing an Applied Biosystems sequencer and dye-labeled terminators. Plasmid DNA was isolated throughout using either Wizard spin preps (Promega) or Qiagen spin preps (Qiagen). The resulting mutant plasmids were transformed into competent *Escherichia coli* DF1020 cells, a PFK-1 deficient strain (*6*, *7*), using the calcium chloride method (*8*).

Protein Purification. Purification of wild-type BsPFK and of all mutant forms of BsPFK was performed according to Valdez et al. (*9*) with minor modifications as described previously (*5*, *10*). Protein concentrations were determined by either BCA or by absorbance using $\epsilon_{280} = 18910\ M^{-1}\ cm^{-1}$ (*4*).

Hybrid Formation and Isolation. Wild-type and modified BsPFK were incubated together in 2 M KSCN and 20 mM Tris-HCl (pH 8.5) for 30 min at room temperature to facilitate breakdown of the parental tetramers to their individual subunits. To improve the yield of the 1:3 hybrid, approximately a 2-fold greater amount of mutant protein than wild-type protein was often used, with a final concentration equal to 2 mg/mL total protein. After incubation, the sample was dialyzed against 20 mM Tris-HCl (pH 9.0) for 3 h at room temperature with two buffer changes after 60 min. The protein mixture was then loaded onto a Pharmacia Mono-Q

[1] Abbreviations: Fru-6-P, fructose 6-phosphate; PFK, phosphofructokinase; BsPFK, phosphofructokinase from *Bacillus stearothermophilus*; PEP, phospho(enol)pyruvate; MOPS, 3-(*N*-morpholino)-propanesulfonic acid; EPPS, *N*-(2-hydroxyethyl)piperazine-*N*′-3-propanesulfonic acid; Tris, tris(hydroxymethyl)aminomethane; MES, 2-(*N*-morpholino)ethanesulfonic acid.

HR 10/10 FPLC anion-exchange column, previously equilibrated with 20 mM Tris-HCl (pH 9.0). Elution was achieved with a linear 0−1 M NaCl gradient. The absorbances at 280 nm and activity assays were performed on the fractions to locate the different hybrid species.

To identify the different hybrid species, the fractions comprising the various protein peaks were pooled together, and a sample was loaded onto a 4% stacking/10% resolving native polyacrylamide gel (*11*) and run for 3 h at 100 V in an ice bath using the Bio-Rad Mini-Protean II electrophoresis system. After electrophoresis, the gels were stained in 0.1% Coomassie blue for approximately 30 min prior to destaining and analysis. The isolated 1:3 hybrid was then stored at 4 °C to prevent rehybridization.

Enzymatic Activity Assays. Activity measurements of BsPFK were conducted by coupling the formation of fructose 1,6-bisphosphate to the oxidation of NADH and monitoring the corresponding decrease in the absorbance at 340 nm. Assays were carried out in a 1.0 mL reaction volume containing 50 mM MES−KOH (pH 6.0), 50 mM MOPS−KOH (pH 7.0), or 50 mM EPPS−KOH (pH 8.0) buffer plus 100 mM KCl, 5 mM $MgCl_2$, 0.1 mM EDTA, 2 mM DTT, 0.2 mM NADH, 250 μg of aldolase, 50 μg of glycerol-3-phosphate dehydrogenase, and 5 μg of triosephosphate isomerase. Creatine kinase and creatine phosphate were added to regenerate MgATP from MgADP to alleviate the activation of BsPFK by MgADP. The concentration of MgATP was held constant at 3 mM in all assays, and the concentrations of Fru-6-P and the inhibitor PEP were adjusted as indicated. Assays were initiated by the addition of 10 μL of BsPFK that had been appropriately diluted so as not to exceed a change of 0.1 absorbance unit at 340 nm per minute. One unit of activity is defined as the production of 1 μmol of fructose 1,6-bisphosphate per minute. Activity measurements were conducted on Beckman Series 600 spectrophotometers using a linear regression calculation to convert change in absorbance at 340 nm to enzyme activity.

Data Analysis. Initial velocity activities as a function of Fru-6-P concentration for the wild-type enzyme were fit to the equation (*12*):

$$v = \frac{V_{max}[A]^{n_H}}{K_{1/2}^{n_H} + [A]^{n_H}} \quad (1)$$

where v equals the steady-state rate of turnover, V_{max} represents the maximal specific activity, [A] equals the concentration of Fru-6-P, $K_{1/2}$ is the concentration of Fru-6-P resulting in half-maximal specific activity, and n_H is the Hill coefficient.

Data obtained from the hybrid enzymes that exhibited two distinct affinities for Fru-6-P were fit to the equation:

$$v = \frac{V_{max}[A]}{K_{1/2} + [A]} + \frac{V'_{max}[A]}{K'_{1/2} + [A]} \quad (2)$$

where V'_{max} and $K'_{1/2}$ refer to the maximal specific activity and apparent dissociation parameters for the low-affinity active site population, respectively. The introduction of nonunitary Hill coefficients into eq 2 did not improve the fit significantly. This result was not surprising since no cooperativity should be associated with the single high-affinity interaction, and saturation of the low-affinity sites could not be completely achieved.

The variation in the apparent $K_{1/2}$ for Fru-6-P as a function of PEP concentration was fit to the equation:

$$K_{1/2} = K_{ia}^0\left(\frac{K_{iy}^0 + [Y]}{K_{iy}^0 + Q_{ay}[Y]}\right) \quad (3)$$

where [Y] represents the concentration of the allosteric inhibitor PEP, K_{ia}^0 is the apparent dissociation constant for the substrate Fru-6-P in the absence of PEP, K_{iy}^0 is the dissociation constant for PEP in the absence of Fru-6-P, and Q_{ay} is the coupling parameter describing the extent to which the binding of PEP effects the binding of Fru-6-P and vice versa as defined by the equation:

$$\frac{K_{ia}^0}{K_{ia}^\infty} = \frac{K_{iy}^0}{K_{iy}^\infty} = Q_{ay} \quad (4)$$

where K_{ia}^∞ and K_{iy}^∞ represent the dissociation constants for Fru-6-P and PEP, respectively, in the saturating presence of the other ligand. By resolving both the terms K_{iy}^0 and Q_{ay}, eq 3 allows the separate quantification of both PEP binding affinity and its allosteric effect once bound, respectively (*4*, *5*, *10*, *13*−*16*).

The coupling parameter, Q_{ay}, describes both the nature and magnitude of the effect the allosteric ligand has upon the binding of the substrate. If $Q_{ay} < 1$, the allosteric ligand is an inhibitor, and if $Q_{ay} > 1$, the allosteric ligand is an activator. If $Q_{ay} = 1$, then the allosteric ligand has no effect on the binding of substrate. In the case of the inhibitor PEP, the smaller the value of Q_{ay}, the greater the extent of inhibition by PEP upon substrate binding.

The coupling parameter can also be used to calculate the free energy associated with the interaction between substrate and allosteric effector, provided the rapid equilibrium assumption is valid as it is for BsPFK (*16*) using the equation:

$$\Delta G_{ay} = -RT \ln Q_{ay} \quad (5)$$

where ΔG_{ay} is the free energy of inhibition by PEP, R is the gas constant expressed in kcal/(deg·mol), and T is absolute temperature in kelvin. Allosteric inhibition is defined by a ΔG_{ay} value greater than zero, while allosteric activation results in a ΔG_{ay} value less than zero. When no coupling between the ligands occurs, $\Delta G_{ay} = 0$.

All data analysis was performed on either a Power Macintosh 7100/80AV or a Macintosh G4 using Kaleidagraph 3.08 (Synergy Software).

RESULTS

Strategy. Oligomeric enzymes often contain binding sites that reside across subunit interfaces. BsPFK follows form, with the added feature that its four active sites are located across one dimer−dimer interface while its four allosteric sites are formed across the other dimer−dimer interface (*17*). Due to the asymmetry of the interaction of the individual subunits, the residues making up a complete binding site [be it an active site capable of binding the substrate fructose 6-phosphate (Fru-6-P) or an allosteric site capable of binding either the inhibitor phospho(enol)pyruvate (PEP) or the

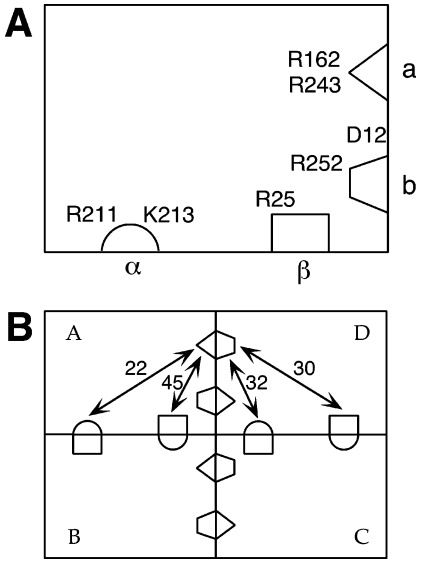

FIGURE 2: (A) Schematic representation of a single subunit of BsPFK. Two complementary halves of the Fru-6-P binding site are denoted by the symbols labeled a and b. The two complementary halves of the allosteric PEP binding site are denoted by the symbols labeled α and *β*. Arginine and lysine residues which were modified to reduce binding affinity are indicated next to the respective binding site. Modification of D12 was also required to facilitate hybrid formation in the presence of the R252A mutations as discussed in the text. (B) Schematic representation of the assembled tetramer of BsPFK. The four unique pairwise heterotropic interactions are depicted and labeled by the distances in angstroms between the sites. Individual subunits are labeled A−D.

activator MgADP] are different on one side compared to the other. This arrangement is depicted schematically in Figure 2. For example, the Fru-6-P binding site contains an arginine at position 162 on one side of the binding cavity (a-side) and an arginine at position 252 on the other side (b-side). Likewise, the allosteric sites are flanked by both an arginine and a lysine at positions 211 and 213, respectively, from one subunit (α-side) and an arginine at position 25 from the neighboring subunit (*β*-side). It is this characteristic of BsPFK which we have exploited to distinguish the different possible ways Fru-6-P and PEP might interact. The four different heterotropic interactions are depicted in a schematic of the fully formed tetramer in Figure 2B. To distinguish the different heterotropic interactions from one another, the distance between a single active site and each of the four allosteric sites was measured according to their locations within the crystal structure (*17*). This results in four unique distances[2] of 22, 30, 32, and 45 Å as indicated in Figure 2B. In this report, the four interactions will be referred to by these distances. However, this notation is not meant to imply anything about the route by which information must travel from one site to another.

As we have shown earlier, an R162E mutation to the a-side of the active site is sufficient to substantially diminish the binding affinity of Fru-6-P (*10*). Similarly, R211E/R213E modifications of the α-side of the allosteric site is sufficient

[2] The structure determined by Shirmer and Evans (*17*) has Fru-6-P bound in the active site and ADP bound in the allosteric site. The distances associated with each heterotropic interaction were measured from the phosphorus atom of the Fru-6-P molecule bound in the active site to each of the *β*-phosphorus atoms of the ADP molecules bound in the allosteric sites.

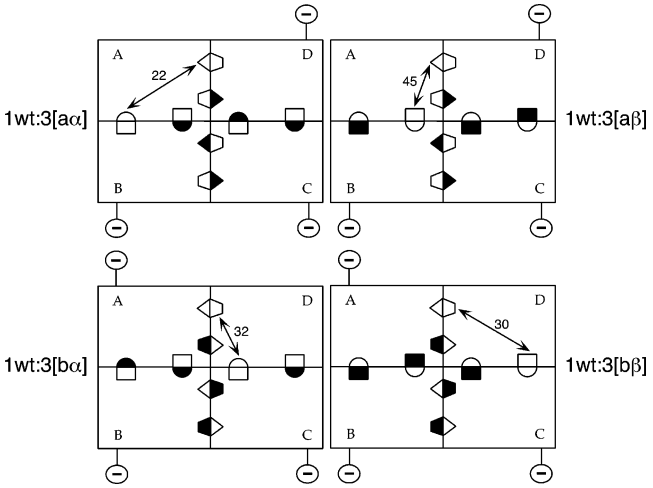

FIGURE 3: Two-dimensional representations of the four BsPFK 1:3 heterotetramers which individually isolate each of the four heterotropic interactions found in the native tetramer that are shown in Figure 2B. Filled shapes indicate the side of the binding site that has been modified to greatly reduce the binding affinity of the respective ligand. The K90E/K91E charge tag that was added to all of the mutant subunits to facilitate separation is also indicated. The specific residues within the active sites and allosteric sites that have been modified in each case are described in the text.

to decrease PEP affinity dramatically (*10*). Variants of BsPFK containing all of these modifications we designate [aα]. We have also developed procedures for constructing and isolating a hybrid form of BsPFK that contains one subunit of wild type and three subunits of [aα], denoted 1wt:3[aα]. This hybrid possesses a single unmodified active site and a single unmodified allosteric site, and the allosteric coupling between these sites has been measured (*10*). An examination of the structure of BsPFK (*17*) reveals that this hybrid isolates the 22 Å interaction.

Below we describe the identification of mutations from the b-side of the active site and the *β*-side of the allosteric site that similarly nearly abolish binding of Fru-6-P and PEP, respectively, without otherwise disrupting the structure substantially. The identification of these mutants has enabled us to construct four different modified enzymes that each exhibit poor binding of both Fru-6-P and PEP: [aα], [b*β*], [a*β*], and [bα]. Construction of 1:3 hybrids with each of these variants has allowed us to isolate each of the four different heterotropic interactions between Fru-6-P and PEP individually.

Figure 3 illustrates the isolation of each of the four possible heterotropic interactions via their respective 1:3 hybrid combinations. The presence of a mutation at a binding site that substantially prevents binding at that site is designated by a filled shape. The native, nonsubstituted portions of binding sites remain open. The arrow drawn between the two remaining completely unmodified binding sites depicts the specific heterotropic interaction isolated within each of the four different 1:3 hybrids. Table 1 lists the four different BsPFK variants used in this study, the modifications they contain, and the specific interaction isolated in the 1:3 hybrid.

b-Side Active Site Mutations. On the b-side of the active site, R252 directly interacts with the 6-phosphate of Fru-6-P according to the X-ray structure (*17*). To discourage Fru-6-P binding, the R252E mutation was introduced. However, this mutation dramatically lowered k_{cat} (data not shown),

Table 1: List of Mutations[a] Used To Isolate the Four Individual Allosteric Heterotropic Interactions in BsPFK

heterotropic interaction isolated	active site (a or b side)	allosteric site (α or β side)
22 Å	R162E (a)	R211E/K213E (α)
30 Å	R252A/D12A (b)	R25E (β)
32 Å	R252A/D12A (b)	R211E/K213E (α)
45 Å	R162E or R243E (a)	R25E (β)

[a] In addition, each variant also contained the charge tag modification K90E/K91E on the surface of the protein to facilitate the separation of the various hybrid species via anion-exchange chromatography as described in the text.

increasing the likelihood that this mutation disrupted the basic structure of the enzyme, so a more conservative mutation, R252A, was constructed. This modification diminished binding by more than 2 orders of magnitude without significantly affecting k_{cat} as previously reported by Valdez et al. (*9*). However, R252A did not properly form hybrids, despite extensive efforts to find suitable conditions. Further examination of the structure revealed that R252 interacts not only with Fru-6-P but also with D12, which in turn interacts with H160 on the adjacent subunit. We reasoned that D12, unrestrained by an interaction with R252, might be perturbed by H160 in such a way so as to interfere with the subunit interface. Consequently, we introduced a second mutation, D12A, which, when combined with R252A, produced a protein that readily formed all possible hybrids with wild type.

Figure 4A illustrates the result of incorporating the R252A/D12A mutations on the activity of the enzyme. Equation 1 was used to fit both the wild-type and mutant data, although the Hill coefficient did not vary significantly from 1. The apparent dissociation of Fru-6-P ($K_{1/2}$) is increased by approximately 240-fold relative to that of wild type. Moreover, the specific activity of the mutant is unaffected, indicating no significant structural perturbation of the active site.

β-Side Allosteric Site Mutations. On the β-side of the allosteric site, R25 was changed to a glutamate. The effects of this mutation are shown in Figure 4B. Due to the difficulties in assessing the direct binding affinity of PEP to BsPFK, the ability of PEP to inhibit the binding of Fru-6-P for both the wild-type and R25E mutant enzymes was measured. The resulting data were fit to eq 3 to assess the affinity of PEP for BsPFK. As Figure 4B shows, it requires more than 10 mM PEP to inhibit the $K_{1/2}$ for Fru-6-P, suggesting a decrease in PEP affinity of nearly 4 orders of magnitude. Table 2 summarizes the kinetic and allosteric properties of the wild-type enzyme and the active site and allosteric site mutant forms of BsPFK, including those characterized previously (*10*).

Isolating the Four Heterotropic Interactions. Having identified these new mutations, R252A/D12A at the b-side of the active site and R25E at the β-side of the allosteric site, and in conjunction with the mutations on the a-side of the active site and α-side of the allosteric site, R162E and R211E/K213E, respectively, four different modified proteins were generated which demonstrated very poor binding of Fru-6-P in the active site and PEP in the allosteric site. These proteins are designated [aα], [aβ], [bα], and [bβ] to indicate

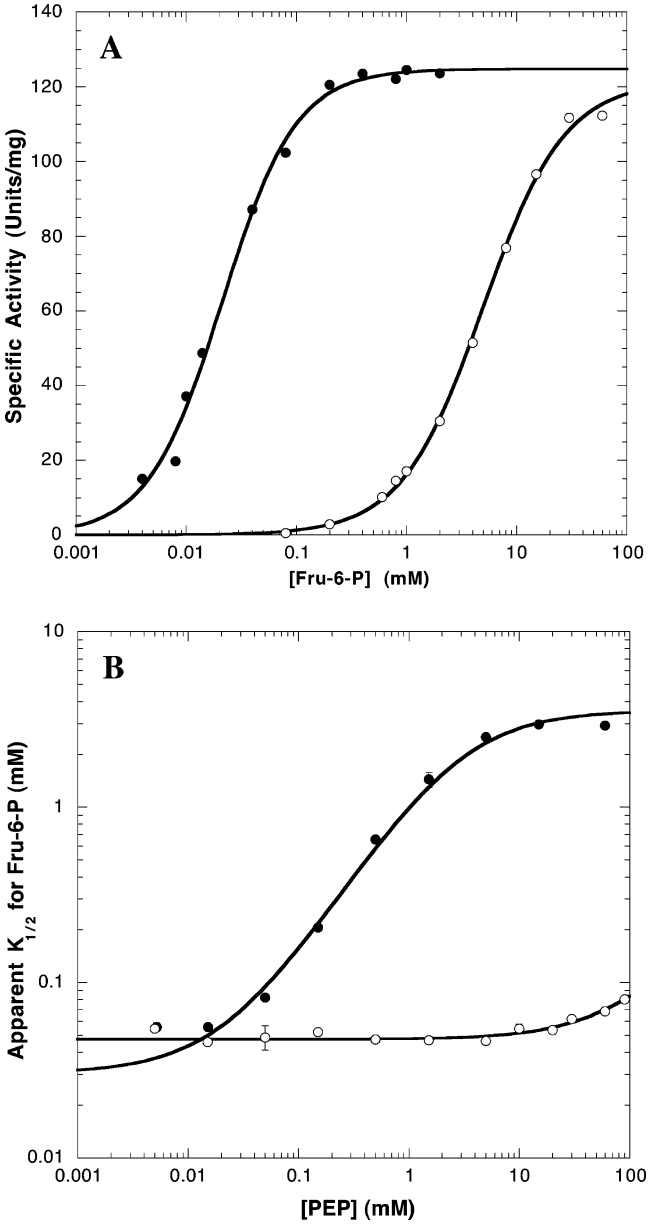

FIGURE 4: Steady-state kinetic experiments to determine the effects of b-side active site and β-side allosteric site mutations on the binding of the substrate Fru-6-P and the inhibitor PEP, respectively. (A) Fru-6-P saturation profiles for wild-type BsPFK (●) and the active site mutant R252A/D12A (○) at pH 7.0 and 25 °C. The MgATP concentration was 3 mM. The curves represent the best fit of these data to eq 1 as described in the text. (B) Dependence of the apparent $K_{1/2}$ for Fru-6-P on increasing concentrations of the inhibitor PEP for wild-type BsPFK (●) and the R25E mutant protein (○) at pH 7.0 and 25 °C. The curves represent the best fit of these data to eq 3 as described in the text. The resulting parameters are summarized in Table 2.

which of the active site and allosteric site mutations they contain. These proteins were further modified by incorporating the K90E/K91E mutations. K90 and K91 occur on the surface of the protein, and these modifications serve to allow separation of the mutant protein from the native protein on anion-exchange chromatography while not interfering in the functional properties of the enzyme (*10*).

Hybrids between each of those four modified proteins and wild type were made following the procedure outlined in Materials and Methods and confirmed by native PAGE. The 1:3 hybrid (wild type:mutant) of each modified protein was

Table 2: Steady-State Kinetic and Thermodynamic Coupling Parameters[a] for Wild-Type BsPFK, the Active Site Mutants, and the Allosteric Site Mutants at 25 °C and pH 7.0 with [MgATP] = 3 mM

enzyme	V_{max} (units/mg)[b]	$K_{1/2}$ (mM)[b]	n_H[b]
wild type	125 ± 2	0.021 ± 0.001	1.30 ± 0.09
R252A/D12A	122 ± 3	5.0 ± 0.3	1.17 ± 0.05
R162E[c]	146 ± 6	21.2 ± 1.9	1.15 ± 0.06
R25E	91 ± 1	0.047 ± 0.002	1.27 ± 0.05
R211E/K213E[c]	109 ± 1	0.058 ± 0.001	1.12 ± 0.08

[a] The values determined for K_{iy}^0 were ~100 mM PEP and ~20 mM PEP for the R25E and R211E/K213E mutant proteins, respectively. [b] Pertaining to Fru-6-P saturation profiles at 0 mM PEP. [c] Experiment performed under identical conditions except at pH 8.0 (*10*).

isolated and purified as described previously (*10*). All 1:3 hybrids were stored at 4 °C, and no rehybridization between subunits was observed for at least 4 weeks as confirmed by native PAGE analysis (data not shown). Examination of the structure of the tetrameric form of the enzyme reveals that the 1:3 hybrids of the [aα], [aβ], [bα], and [bβ] proteins isolate the 22, 45, 32, and 30 Å heterotropic interactions, respectively. Isolation and identification of each hybrid were analogous to the results previously described for the [aα] hybrid (*10*).

Functional Properties of the Hybrid Enzymes. The dependence of enzyme activity as a function of Fru-6-P concentration was determined for the wild-type enzyme, as well as the individual 1:3 hybrid species at pH 6.0, 7.0, and 8.0. As expected, the Fru-6-P saturation profiles for the 1:3 hybrids exhibited the saturation of two different types of binding sites, corresponding to the high-affinity and low-affinity active sites, respectively (data not shown). This agrees with previous results reported by Kimmel and Reinhart (*10*) for the 22 Å interaction at pH 8.0. Data obtained from the Fru-6-P saturation profiles for the wild-type enzyme were fit to eq 1, while data for the 1:3 hybrids were fit to eq 2.

Table 3 summarizes the kinetic parameters obtained from these fits for wild-type BsPFK and both the high-affinity (native) and low-affinity (mutated) Fru-6-P binding sites found in the 1:3 hybrids. At all pH values, the maximal specific activity for the high-affinity interaction (V_{max}) is approximately one-fourth that of wild type. This result was expected, as each 1:3 hybrid contains one-fourth the number of native active sites found within the BsPFK tetramer. Also, the maximal specific activity for each of the 1:3 hybrids increases with an increase in pH, a behavior consistent with the wild-type enzyme (*16*). The values obtained for the high-affinity $K_{1/2}$ for Fru-6-P agree, within error, with the $K_{1/2}$ values for the wild-type enzyme except for the 32 Å interaction at pH 8.0. This overall agreement was expected because the wild-type enzyme exhibits little to no cooperativity between active sites in the absence of effector (*18*). We do not have an explanation for the increased value exhibited by the 32 Å interaction at pH 8; however, this perturbation does not seem to adversely affect the allosteric couplings (see below).

The values obtained for the low-affinity active sites also conform to expected results. The maximal specific activities for the three low-affinity active sites (V'_{max}) is approximately three-fourths the V_{max} value for the mutant tetramer, which is comparable to three-fourths the V_{max} value for the wild-type enzyme since the active site mutations do not alter the k_{cat} of BsPFK. Furthermore, the low-affinity $K_{1/2}$ values are generally comparable to the $K_{1/2}$ values measured for the corresponding active site mutant enzymes.

To measure the nature and magnitude of the allosteric effect resulting from each heterotropic interaction, the high-affinity $K_{1/2}$ for Fru-6-P was determined as a function of PEP concentration for each of the four 1:3 hybrids at various pH values. Ideally, this measured allosteric effect would correspond to the interaction of only the native active site and native allosteric site. However, it was previously found that the binding of PEP at high concentration to the three mutated allosteric sites still has the ability to influence the binding of Fru-6-P to the 1:3 hybrid to a small degree (*10*). Consequently, a control hybrid for each 1:3 hybrid was made. This control hybrid consists of one native active site, three mutated active sites, and four mutated allosteric sites. Using the notation introduced by Fenton and Reinhart (*19*), this control hybrid is designated 1|0, where 1 equals the number of native Fru-6-P binding sites and 0 equals the number of native allosteric sites in the tetramer. Thus, we have created two types of 1:3 hybrids in each case, the experimental that isolates a single heterotropic interaction between a native active site and a native allosteric site, designated 1|1, and a control in which the influence of the mutated allosteric sites on a single native active site can be assessed, designated 1|0. Each of the four control hybrids was constructed by substituting the appropriate allosteric site mutant for the wild-type parental protein (*10*). Fru-6-P titrations at pH 6.0, 7.0, and 8.0 were performed for each 1:3 hybrid and its corresponding control hybrid at increasing concentrations of PEP. The measured high-affinity $K_{1/2}$ for each 1|1 hybrid was corrected for the possible influence of PEP binding to the mutated sites by measuring the $K_{1/2}$ for the 1|0 control and then using the equation:

$$K_{1/2}(\text{corrected}) = \frac{K_{1/2}(1|1)}{K_{1/2}(1|0)} \quad (6)$$

In all cases $K_{1/2}(1|0)$ values were independent of PEP concentration except at very high values, as shown previously (*10*).

Figure 5 shows the corrected values for the $K_{1/2}$ for Fru-6-P plotted as a function of PEP concentration at each of the three pH values investigated. With the exception of the 30 Å interaction at pH 6.0 and the 45 Å interaction at all pH values, the high-affinity binding site of each of the 1:3 hybrids was found to behave like the wild-type enzyme in that the addition of PEP increases the $K_{1/2}$ for Fru-6-P in a saturable manner. The coupling between Fru-6-P and PEP in each case, Q_{ay}, was obtained by fitting these data to eq 3, and the results are presented in Table 4. Q_{ay} for each of the 1:3 hybrids is reduced to different extents relative to wild type. Moreover, all of the heterotropic interactions, with the exception of the 45 Å interaction, display an increase in coupling with an increase in pH, a phenomenon consistent with the behavior exhibited by the wild-type enzyme (*16*). Table 4 also presents the coupling data in terms of free energy as calculated by eq 5.

Only the 45 Å heterotropic interaction was found to produce no allosteric effect upon the binding of PEP at any

Table 3: Steady-State Kinetic Parameters for Wild-Type BsPFK and the Four 1:3 Hybrids Containing the Four Individual Allosteric Interactions within BsPFK at 25 °C, pH 6.0, 7.0, and 8.0, [MgATP] = 3 mM, and [PEP] = 0 mM

	high affinity		low affinity	
enzyme	V_{max} (units/mg)	$K_{1/2}$ (mM)	V_{max} (units/mg)	$K_{1/2}$ (mM)
pH 6.0				
wild type	67.1 ± 1.1	0.032 ± 0.001	n/a	n/a
22 Å interaction	22.5 ± 0.5	0.028 ± 0.002	85 ± 1	3.6 ± 0.1
30 Å interaction	15.4 ± 0.4	0.035 ± 0.003	36 ± 1	8.0 ± 0.3
32 Å interaction	14.5 ± 0.5	0.031 ± 0.003	46 ± 2	10.0 ± 0.8
45 Å interaction (R162E)	19.4 ± 1.1	0.039 ± 0.007	85 ± 1	6.2 ± 0.3
45 Å interaction (R243E)	17.6 ± 0.8	0.028 ± 0.004	50 ± 1	5.7 ± 0.5
pH 7.0				
wild type	125 ± 2	0.021 ± 0.001	n/a	n/a
22 Å interaction	28.0 ± 1.0	0.029 ± 0.004	113 ± 2	8.6 ± 0.5
30 Å interaction	26.7 ± 0.7	0.020 ± 0.002	96 ± 3	12.1 ± 0.7
32 Å interaction	30.9 ± 1.1	0.047 ± 0.005	94 ± 3	9.6 ± 0.5
45 Å interaction (R162E)	29.2 ± 0.8	0.024 ± 0.002	114 ± 1	9.3 ± 0.4
45 Å interaction (R243E)	28.0 ± 1.3	0.017 ± 0.003	95 ± 2	6.3 ± 0.5
pH 8.0				
wild type	153 ± 3	0.034 ± 0.001	n/a	n/a
22 Å interaction	36 ± 1	0.034 ± 0.004	90 ± 3	25 ± 2
30 Å interaction	37 ± 2	0.079 ± 0.008	ud[a]	ud
32 Å interaction	38 ± 2	0.310 ± 0.035	ud	ud
45 Å interaction (R162E)	39 ± 1	0.038 ± 0.003	123 ±10	42 ± 6
45 Å interaction (R243E)	39 ± 2	0.024 ± 0.004	117 ± 3	8.3 ± 0.9

[a] ud = undetermined.

Table 4: Thermodynamic Parameters for Wild-Type and the Four Individual Allosteric Interactions (Control Subtracted) at 25 °C, pH 6.0, 7.0, and 8.0, and [MgATP] = 3 mM

enzyme	K^0_{ia} (mM)	K^0_{iy} (mM)	Q_{ay}	ΔG_{ay} (kcal/mol)
pH 6.0				
wild type	0.032 ± 0.001	0.026 ± 0.002	0.041 ± 0.002	1.89 ± 0.03
22 Å interaction	0.026 ± 0.002	0.091 ± 0.086	0.50 ± 0.08	0.41 ± 0.10
30 Å interaction	0.035 ± 0.003	ud[a]	1.00 ± 0.10	0.00 ± 0.006
32 Å interaction	0.029 ± 0.005	0.0045 ± 0.0061	0.56 ± 0.10	0.34 ± 0.10
45 Å interaction (R162E)	0.037 ± 0.004	ud	1.00 ± 0.15	0.00 ± 0.09
45 Å interaction (R243E)	0.033 ± 0.006	0.27 ± 0.08	0.68 ± 0.18	0.23 ± 0.14
pH 7.0				
wild type	0.030 ± 0.002	0.023 ± 0.002	0.0085 ± 0.0004	2.82 ± 0.03
22 Å interaction	0.023 ± 0.002	0.079 ± 0.047	0.33 ± 0.05	0.66 ± 0.10
30 Å interaction	0.019 ± 0.004	0.0003 ± 0.0007	0.59 ± 0.11	0.31 ± 0.11
32 Å interaction	0.035 ± 0.006	0.003 ± 0.002	0.38 ± 0.07	0.57 ± 0.10
45 Å interaction (R162E)	0.024 ± 0.001	ud	1.00 ± 0.06	0.00 ± 0.03
45 Å interaction (R243E)	0.022 ± 0.005	0.04 ± 0.02	0.77 ± 0.18	0.18 ± 0.14
pH 8.0				
wild type	0.027 ± 0.001	0.039 ± 0.001	0.0020 ± 0.0001	3.58 ± 0.02
22 Å interaction	0.031 ± 0.002	0.22 ± 0.07	0.08 ± 0.02	1.48 ± 0.15
30 Å interaction	0.074 ± 0.014	0.002 ± 0.001	0.44 ± 0.08	0.49 ± 0.11
32 Å interaction	0.31 ± 0.06	0.0004 ± 0.0003	0.25 ± 0.05	0.82 ± 0.12
45 Å interaction (R162E)	0.038 ± 0.001	ud	1.00 ± 0.04	0.00 ± 0.02
45 Å interaction (R243E)	0.026 ± 0.003	2.0 ± 0.9	0.78 ± 0.24	0.17 ± 0.20

[a] ud = undetermined.

of the pH values examined. To confirm that this observation was not due to damage to the protein introduced by the mutations, a second mutant protein was constructed in which the active site mutation of R162E was replaced with R243E. R243 is a residue adjacent to R162 on the a-side of the active site. The steady-state characterization of the R243E mutation showed it to be functionally analogous to the R162E mutation (data not shown), and 1:3 hybrids (both 1|1 and 1|0) made with an enzyme containing all of the same mutations in the modified subunits except for the substitution of R243E for R162E likewise behaved similarly in the absence of PEP (see Table 3).

In this case a small, barely significant, coupling was evident at pH 8, which increased as pH decreased to a more significant, but still small value at pH 6. These results are also included in Table 4.

The values of each individually isolated interaction, expressed as coupling free energies, are compared in Figure 6. At pH 8, the 22 Å interaction clearly dominates the values of the other interactions, measuring 1.5 kcal/mol or approximately 42% of the 3.6 kcal/mol coupling free energy of the wild-type tetramer under identical conditions. The 32 and 30 Å interactions have smaller, but significant, values that are approximately one-half and one-third the value at 22 Å, respectively. The 45 Å interaction at best makes only a minor contribution relative to the magnitudes of the other couplings.

The overall trend with pH evident in Figure 6 is consistent with the influence that pH has on the wild-type enzyme, with each coupling individually diminishing in magnitude with lower pH, with the possible exception of the 45 Å coupling. At pH 6, all of the couplings are very small, with the 22 Å

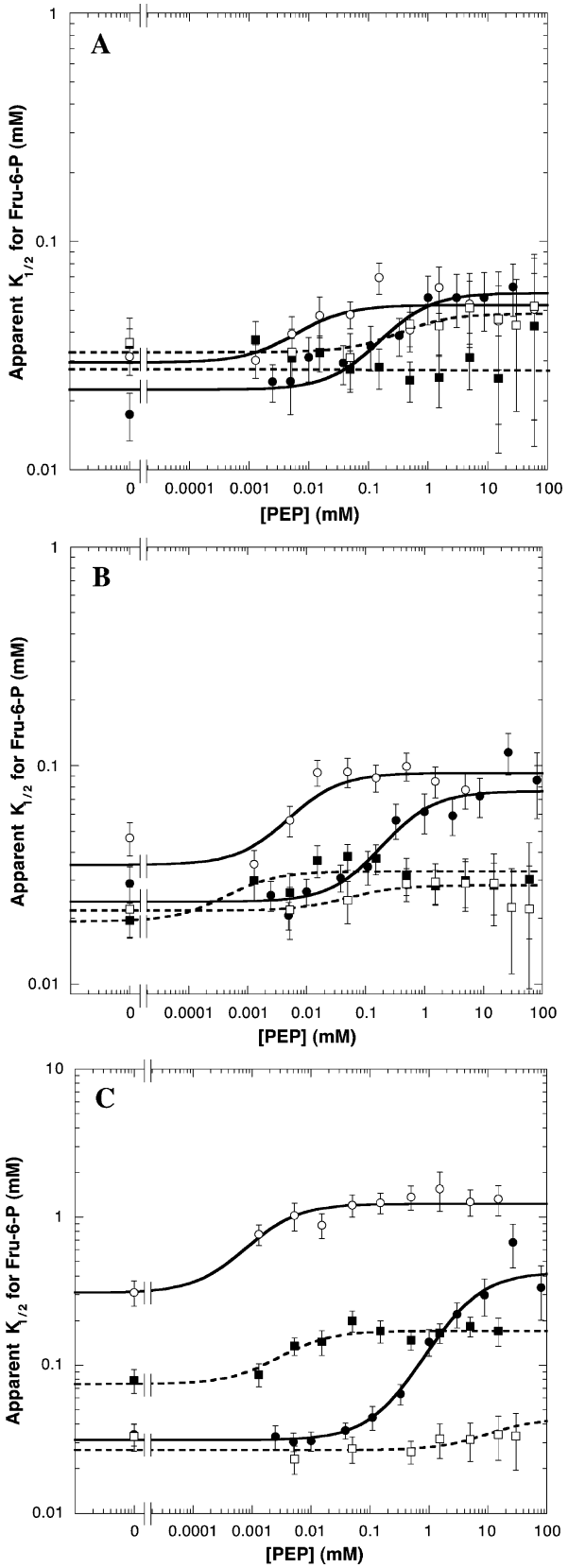

FIGURE 5: Dependence of the corrected apparent $K_{1/2}$ for Fru-6-P on increasing concentrations of the inhibitor PEP for the 22 Å interaction (●), the 30 Å interaction (■), the 32 Å interaction (○), and the 45 Å interaction (□). The hybrids which isolated the 45 Å interaction contained the R243E active site mutation in the modified subunits as described in the text. All of the curves correspond to the best fit of these data to eq 3 as described in the text. Conditions: (A) pH 6.0 (50 mM MES−KOH buffer); (B) pH 7.0 (50 mM MOPS−KOH); (C) pH 8.0 (50 mM EPPS−KOH).

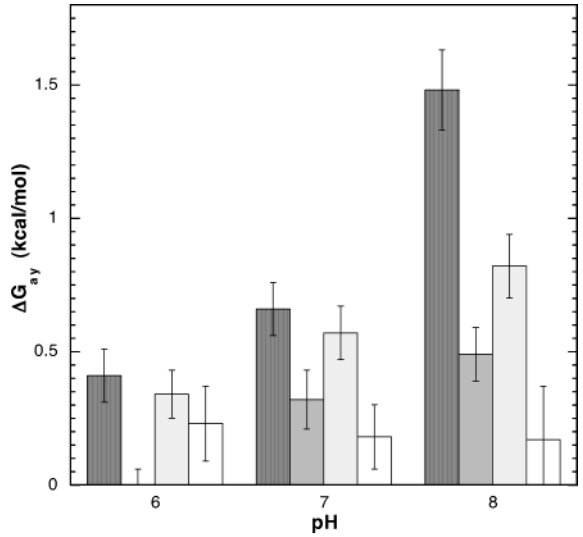

FIGURE 6: Comparison of the individual coupling free energies determined for the four heterotropic interactions at pH 6.0, 7.0, and 8.0. Key: black, 22 Å interaction; dark gray, 30 Å interaction; light gray, 32 Å interaction; white, 45 Å interaction.

coupling being reduced to 0.4 kcal/mol, a value only slightly larger than the 32 Å coupling, while the 30 Å coupling has been reduced to completely negligible values. The 45 Å coupling measured with the R243E mutation is slightly larger than its value at pH 8, and the value determined with the R162E mutation, but the magnitude of the relative error suggests that the significance is marginal.

The question naturally arises whether the differences between the values of the couplings measured in this way are due to intrinsic differences in the couplings as they are manifested in the native tetramer or whether they are created by the structural perturbations that have been introduced in their isolation. To assess this issue, it is necessary to consider the sum of the individual heterotropic coupling free energies and compare that sum to the overall heterotropic coupling functioning in the wild-type tetramer.

The basis for comparing the sum of the individual couplings to the overall coupling comes from the principle of thermodynamic linkage (*20*−*24*). A detailed examination of the origins of overall heterotropic coupling in a dimer (*24*), however, has revealed that changes in homotropic cooperativity, with respect to either substrate or allosteric ligand, introduced by the presence of the heterotropic ligand can also contribute to the magnitude of the apparent heterotropic interaction. Although Fru-6-P binds to BsPFK with little or no cooperativity, positive cooperativity in PEP binding has been observed (*4*). To estimate the total heterotropic interaction that is manifest by the tetrameric enzyme in the absence of cooperative interactions between the several PEP binding sites, we constructed a hybrid between the wild type and a variant containing only the β-side allosteric site and charge tag mutations (K90E/K91E). The 1:3 hybrid was isolated as outlined above, resulting in an enzyme with four native active sites and only one native allosteric site, designated 4|1. This control hybrid does not exhibit PEP binding cooperativity, as expected (data not shown). By analogy to the dimeric case, the overall heterotropic coupling exhibited by the 4|1 hybrid should in principle be one-fourth that observed for the 4|4 wild-type protein in the absence of homotropic cooperativity (*22*, *23*).

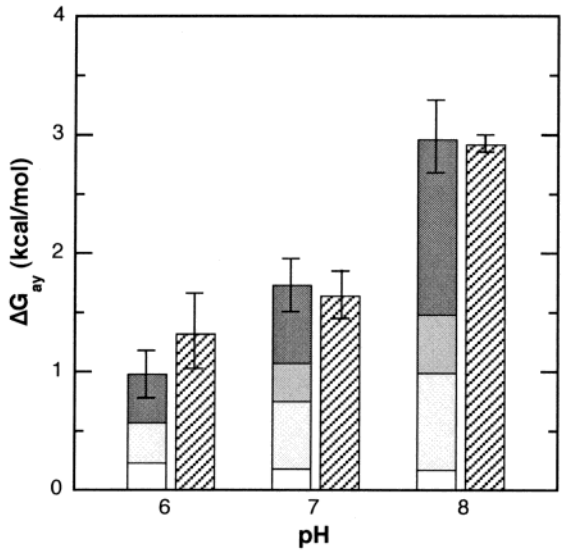

FIGURE 7: Comparison of the sum of the individual coupling free energies determined for the four heterotropic interactions to the overall heterotropic coupling free energy determined from the 4|1 control hybrid at pH 6.0, 7.0, and 8.0. The bar on the left at each pH indicates the sum of the coupling free energies determined individually for the 22 Å interaction (black), the 30 Å interaction (dark gray), the 32 Å interaction (light gray), and the 45 Å interaction (white). The striped bar on the right at each pH corresponds to the coupling free energy determined from the 4|1 control hybrid as described in the text. The latter values should correspond to the total heterotropic coupling in the native tetramer in the absence of homotropic interactions.

A value equal to 4 times the coupling free energy measured for the 4|1 hybrid is presented in Figure 7 , enabling a comparison of this value to the sum of the individual couplings measured in the four 1|1 hybrids. At pH 8.0 and 7.0 these values are in complete agreement. At pH 6.0, the sum is 75% of the control hybrid value, but the relative errors are large enough to make this discrepancy of questionable significance.

DISCUSSION

The agreement of the sum of the measured individual couplings with the 4|1 control hybrid provides strong evidence that the individual interactions isolated in the respective 1:3 hybrids can be related directly to the corresponding interactions as they exist in the native tetramer. At first glance it might not be apparent how these individual couplings, determined with only a single equivalent of each ligand bound, are relevant to the overall heterotropic inhibition of the native tetramer, with four equivalents of each ligand, even ignoring complications that arise from homotropic interactions. Our expectations arise by analogy to the relationship of these individual pairwise couplings to the overall allosteric effect in a homodimer.

Despite the fact that the overall effect of an allosteric ligand in a homodimer requires two equivalents of each ligand to bind, thermodynamic linkage predicts that the overall coupling, Q, measured will be equal to (*24*)

$$Q = Q_{ay1}Q_{ay2}\left(\frac{Q_{yy/a}}{Q_{yy}}\right)\left(\frac{Q_{aa/yy}}{Q_{aa}}\right)^{0.5} \qquad (7)$$

where Q_{ay1} and Q_{ay2} represent the two different individual pairwise couplings and the terms in the parentheses relate to homotropic interactions. In the absence of homotropic interactions, the quantities in the parentheses equal 1. Therefore, the somewhat surprising result, embodied in eq 7, is that the overall allosteric effect is given by the product of the individual coupling parameters. Converting these parameters to coupling free energies using eq 5 leads to the conclusion that the overall allosteric effect in free energy terms is given by the sum of these individual coupling free energies.

By extension, the overall inhibition of the BsPFK tetramer should equal the sum of the individual, unique pairwise couplings in the absence of homotropic effects. Since wild-type PFK does exhibit homotropic cooperativity in the binding of PEP (*4*), a more valid comparison is made to the overall inhibition manifest in the 4|1 hybrid tetramer. This hybrid has only one PEP binding site, removing the opportunity for homotropic effects. Since this hybrid has only one copy of each interaction, not four copies of each like the wild-type enzyme, the expectation is that the overall inhibition exhibited by this tetramer would be one-fourth (in free energy terms) of the heterotropic effects contributing to the behavior of the wild-type enzyme. Consequently, the contribution of the heterotropic interactions to the apparent inhibition by PEP in the wild-type enzyme can be estimated to be equal to 4 times the inhibition observed in the 4|1 hybrid. Since the individual couplings add up to the total heterotropic effect deduced from the behavior of the 4|1 hybrid as shown in Figure 7, the pairwise couplings isolated in the various 1|1 hybrids likely reflect the corresponding interactions in the wild-type enzyme.

It is significant, therefore, that the value of each of the couplings is different. Moreover, as pH is varied, not only do the absolute values of the couplings change but also their relative values, indicating that the binding of a single Fru-6-P equivalent is influenced to a unique extent depending on which of the four allosteric sites is occupied by PEP. We note that our data do not indicate how a second equivalent of bound PEP might further influence the binding of that first Fru-6-P equivalent. Nonetheless, this result clearly lies between the predictions made by either a simple concerted model or a simple sequential model, such as summarized in Figure 1.

It is also unlikely, given the modest magnitudes of the individual couplings even at pH 8, that a single species containing one bound PEP and one bound Fru-6-P would be formed in a suitable titration experiment. Although one would clearly expect the concentration of the species with Fru-6-P and PEP 45 Å apart to dominate (except at pH 6), the other species would be populated to lesser, but nonzero, extents at ambient temperatures, especially at the lower pH values. Thus a two-state view of the structural response of BsPFK to ligand binding becomes far too limiting a way of modeling its functional behavior, even in the seemingly simple case of the binding of a single equivalent of each ligand.

These results also suggest that allosteric interactions proceed by different pathways when considering how different sites are coupled. Stated another way, it is now reasonable to attempt to define the residues that are responsible for transmitting the influence between the various pairs of active and allosteric sites. Furthermore, it is unlikely

that the same residues will be important for establishing the allosteric conduit in each case. Since the hybrids isolate each individual interaction, however, determination of the residues that participate in the transmission of the allosteric influence would now seem to be possible, and these investigations are ongoing.

REFERENCES

1. Monod, J., Wyman, J., and Changeux, J. P. (1965) *J. Mol. Biol. 12*, 88−118.
2. Koshland, D. E., Jr., Nemethy, G., and Filmer, D. (1966) *Biochemistry 5*, 365−385.
3. Hengartner, H., and Harris, J. L. (1975) *FEBS Lett. 55*, 282−285.
4. Riley-Lovingshimer, M. R., and Reinhart, G. D. (2001) *Biochemistry 40*, 3002−3008.
5. Kimmel, J. L., and Reinhart, G. D. (2000) *Proc. Natl. Acad. Sci. U.S.A. 97*, 3844−3849.
6. Daldal, F. (1983) *J. Mol. Biol. 168*, 285−305.
7. Hellinga, H. W., and Evans, P. R. (1985) *Eur. J. Biochem. 149*, 363−373.
8. Cohen, S. N., Chang, A. C. Y., and Hsu, L. (1972) *Proc. Natl. Acad, Sci. U.S.A. 69*, 2110.
9. Valdez, B. C., French, B. A., Younathan, E. S., and Chang, S. H. (1989*) J. Biol. Chem. 264*, 131−135.
10. Kimmel, J. L., and Reinhart, G. D. (2001) *Biochemistry 40*, 11623−11629.
11. Laemmli, U. K. (1970) *Nature 27*, 680.
12. Hill, A. V. (1910) *J. Physiol. (London) 40*, iv−vii.
13. Tlapak-Simmons, V. L., and Reinhart, G. D. (1998) *Arch. Biochem. Biophys. 308*, 226−230.
14. Johnson, J. L., and Reinhart, G. D. (1994) *Biochemistry 33*, 2635−2643.
15. Johnson, J. L., and Reinhart, G. D. (1997) *Biochemistry 36*, 12814−12822.
16. Tlapak-Simmons, V. L., and Reinhart, G. D. (1998) *Biophys. J. 75*, 1010−1015.
17. Schirmer, T., and Evans, P. R. (1990) *Nature 343*, 140−151.
18. Evans, P. R., and Hudson, P. J. (1979) *Nature 279*, 500−504.
19. Fenton, A. W., and Reinhart, G. D. (2002) *Biochemistry 41*, 13410−13416.
20. Wyman, J. (1964) *Adv. Protein Chem. 19*, 223−286.
21. Wyman, J. (1967) *J. Am. Chem. Soc. 89*, 2202−2218.
22. Weber, G. (1972) *Biochemistry 11*, 864−878.
23. Weber, G. (1975) *Adv. Protein Chem. 29*, 1−83.
24. Reinhart, G. D. (1988) *Biophys. Chem. 30*, 159−172.

BI035077P